Short-Term Characterization of Building Integrated Photovoltaic Panels

By

A. Hunter Fanney, Brian P. Dougherty
And Mark W. Davis

National Institute of Standards and Technology
Building and Fire Research Laboratory
Heat Transfer and
Alternative Energy Systems Group
Gaithersburg, MD 20899-8632 USA

Reprinted from Transactions of the ASME, the Journal of Solar Energy Engineering, Vol. 125, No.2, pp. 13-20, February 2003

NIST
National Institute of Standards and Technology

Short-Term Characterization of Building Integrated Photovoltaic Panels*

A. Hunter Fanney
e-mail: Hunter.Fanney@nist.gov

Brian P. Dougherty

Mark W. Davis

National Institute of Standards and Technology,
100 Bureau Drive, MS 8632,
Gaithersburg, MD 20899-8632

Building integrated photovoltaics, the integration of photovoltaic cells into one or more exterior building surfaces, represents a small but growing part of today's $2 billion dollar photovoltaic industry. A barrier to the widespread use of building integrated photovoltaics (BIPV) is the lack of validated predictive simulation tools needed to make informed economic decisions. The National Institute of Standards and Technology (NIST) has undertaken a multi-year project to compare the measured performance of BIPV panels to the predictions of photovoltaic simulation tools. The existing simulation models require input parameters that characterize the electrical performance of BIPV panels subjected to various meteorological conditions. This paper describes the experimental apparatus and test procedures used to capture the required parameters. Results are presented for custom fabricated mono-crystalline, polycrystalline, and silicon film BIPV panels and a commercially available triple junction amorphous silicon panel. [DOI: 10.1115/1.1531642]

Introduction

The National Institute of Standards and Technology has undertaken a multi-year project to validate and improve, if needed, computer simulation tools used to predict the energy production of building integrated photovoltaic panels [1]. These tools will enable building owners and designers to accurately quantify the economic savings associated with building integrated photovoltaic panels.

Among the models available for predicting the performance of photovoltaic systems are PV-Design Pro [2], developed jointly by Maui Solar Software Corporation and Sandia National Laboratories (SNL), and PHotovoltaic ANalysis and TrAnsient Simulation Method (PHANTASM) [3] developed by the University of Wisconsin's Solar Energy Laboratory. Researchers at SNL have also developed PVMOD, a model used within SNL to predict the performance of a wide variety of photovoltaic systems.

Input parameters required by these models include the photovoltaic panels' current and voltage at maximum power conditions, open circuit voltage, short circuit current, number of cells in series within a module, and the temperature coefficients associated with the short circuit current and open circuit voltage. The PHANTASM model also requires the nominal operating cell temperature, the glazing material's solar transmittance, the photovoltaic cell's solar absorptance, and the electrical band-gap of the photovoltaic material. Additional PV-Design Pro input parameters include the maximum power voltage and current temperature coefficients and the polynomials that are used to predict the panel's electrical performance response to changes in incident angle and absolute air mass.

NIST has constructed an outdoor solar tracking test facility to obtain the needed parameters. This paper describes the experimental apparatus, test procedures used to obtain the various parameters, and the resulting measurements. Results are compared to data, if available, from manufacturers and the Sandia National Laboratories.

*Received the Best Paper Award from the Photovoltaics Technical Committee of the Solar Energy Division at the *2002 Solar Conference*, in Reno, Nevada, in June 2002.

Contributed by the Solar Energy Division of THE AMERICAN SOCIETY OF MECHANICAL ENGINEERS for publication in the ASME JOURNAL OF SOLAR ENERGY ENGINEERING. Manuscript received by the ASME Solar Energy Division, February 2002; final revision, August 2002. Associate Editor: A. Reddy.

Experimental Apparatus

BIPV Panel Description. The panels selected for characterization include custom-fabricated mono-crystalline, polycrystalline, and silicon film BIPV panels and a commercially available triple-junction amorphous silicon module (Table 1). The selected panels are duplicates of those installed in NIST's BIPV "test bed" [4]. The custom fabricated panels were made to NIST specifications by a firm that specializes in BIPV panels for commercial and residential applications. Design considerations included incorporating borders that minimize shading on the cells, the use of readily available cells, and cell interconnections that resulted in electrical configuration compatible with the monitoring equipment.

The rated power values listed in Table 1 for the moncrystalline, polycrystalline, and silicon film panels are based upon *flash tests* performed by the fabricator. The amorphous silicon BIPV panel rating is taken from the manufacturer's literature. Three different areas are listed in Table 1: cell, aperture, and coverage. Cell area is defined as the number of cells within a panel times the area of each individual cell. The aperture area is the sunlit opening in the building wall prior to adding the sashing required to mount the BIPV panels. Coverage area is the portion of each panel covered by cells including the spaces between adjacent cells.

With the exception of the triple-junction amorphous panels, which was commercially available, the costs listed in Table 1 are the per panel costs based on producing four panels using each cell technology. The triple-junction amorphous panel was constructed using two commercially available modules connected in series. It should be noted that the costs given in Table 1 reflect the fact that the amorphous panels were off-the-shelf items whereas the other panels were custom fabricated.

Solar Tracking Test Facility. A mobile solar tracking facility is used to characterize the electrical performance of building integrated photovoltaic panels, Fig. 1. Software has been developed for the mobile solar tracker that allows the user to select the following tracking modes:

- Azimuth and elevation tracking
- Azimuth tracking
- Elevation tracking
- Azimuth tracking with user selected offset
- Elevation tracking with user selected offset
- User selected incident angle tracking

Table 1 Building integrated photovoltaic panel specifications

Cell Technology	Mono Crystalline	Poly Crystalline	Silicon Film	Triple-Junction Amorphous
Panel Dimensions (m×m)	1.38×1.18	1.38×1.18	1.38×1.18	1.37×1.48
Front Cover	6 mm glass	6 mm glass	6 mm glass	2 mm* Tefzal
Encapsulant	EVA	EVA	EVA	EVA
Backsheet/Color	*Tedlar/Charcoal	Tedlar/Charcoal	Tedlar/Charcoal	Stainless Steel
Cell dimensions (mm×mm)	125×125	125×125	150×150	119×340
Number of Cells (in series)	72	72	56	44
Adjacent Cell Spacing (mm)	2	2	2	
Vertical Border Width (mm)	100	100	51	8
Top Border Height (mm)	72	72	55	11
Bottom Border (mm)	70	70	29	5
Recessed Distance to PV Cell (mm)	12	12	12	9
Glazing Covered by PV Cells %	63	69	80	88
Total Cost ($)	1324	1123	995	578
Price/Watt ($/W)	8.66	8.43	10.75	4.52
Rated Power (W)	153	133	93	128
Cell Area (m^2)	1.020	1.128	1.341	1.780
Aperture Area (m^2)	1.682	1.682	1.682	2.108
Coverage Area (m^2)	1.160	1.160	1.371	1.815

*Certain trade names and company products are mentioned in the test or identified in an illustration in order to adequately specify the experimental procedure and equipment used. In no case does such an identification imply recommendation or endorsement by the National Institute of Standards and Technology, nor does it imply that the products are necessarily the best available for the purpose.

The mobile solar tracking facility incorporates meteorological instruments, a data acquisition system, and a photovoltaic curve tracer. Precision spectral pyranometers are used to measure total (beam plus diffuse) solar radiation. Two instruments are used to provide redundant measurements. A pyrheliometer is used to measure the beam component of solar radiation. Long-wave radiation, greater than 3 μm, is measured using a precision infrared radiometer. Spectral radiation data from 300 nm to 1100 nm is obtained using a spectroradiometer with selectable scan intervals of 1 nm, 2 nm, 5 nm, or 10 nm.

A propeller-type sensor and wind vane assembly is used to measure wind speed and direction. Ambient temperature is measured using a perforated tip, type-T thermocouple sensor enclosed in a naturally ventilated multi-plate radiation shield.

The output signals of the meteorological instruments and thermocouples associated with the building integrated photovoltaic panels are measured using a data acquisition system. The data acquisition system incorporates a 6.5-digit multi-meter, IEEE 488 and RS 232 interfaces, and multiplexing relay cards that can accommodate up to 60 transducers. Although the multiplexer cards have built-in thermocouple reference junctions, improved accuracy is obtained through the use of an electronic ice point reference.

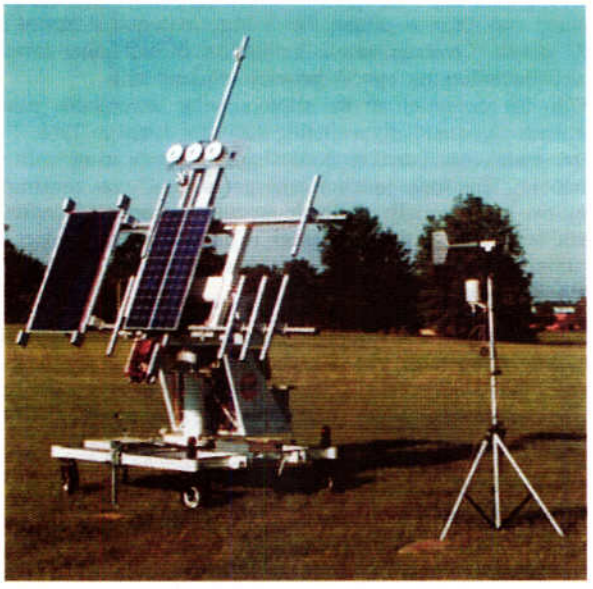

Fig. 1 NIST's Mobile Solar Tracking Facility

The solar tracker incorporates an IV curve tracer to capture the electrical performance of the panel being evaluated. The curve tracer is programmed to sweep the panel's IV curve and store the resulting values every minute. Although the curve tracer incorporates two voltage ranges (60 V and 600 V) and two current ranges (10 A and 100 A), to date, the lower current and voltage ranges have been used resulting in voltage and current resolutions of 14 mV and 2.4 mA, respectively.

The solar tracking test facility is powered by means of an onboard uninterruptible power supply (UPS) capable of operating the equipment for approximately 14 hr. For multiple day tests, the UPS is charged through the use of a portable generator.

Test Procedures

The simulation models' input parameters are obtained using the solar tracking facility and various test procedures. A description of each input parameter and the test procedure used to obtain it follows.

Temperature Coefficients. Temperature coefficients are used to quantify the relationship between various electrical characteristics of a photovoltaic device and its operating temperature. The computer simulation models use temperature coefficients to translate the electrical output of a photovoltaic panel at a given reference temperature to the electrical output at the panel's operating temperature. Temperature coefficients for the short-circuit current, the open circuit voltage, maximum power current, and maximum power voltage are measured for each building integrated photovoltaic panel.

Open-circuit voltage and short-circuit current temperature coefficients are addressed within ASTM E 1036M [5]. The correction factors within this test method are determined from a matrix of open-circuit voltage and short-circuit current values that result from measurements of the device over a range of operating temperatures and incident irradiances. The test procedure states that the measurements should be made over temperature and irradiance ranges of 0–80°C and 800–1000 W/m^2, respectively.

Although ASTM E 1036M suggests that the measurements be made using a pulsed indoor solar simulator, the temperature coefficients for this study were determined outdoors using the NIST mobile solar tracking facility. Outdoor, as opposed to indoor, test-

ing was selected for a number of reasons. A temperature-controlled pulsed indoor solar simulator, sufficient in size to test the 1.38 m×1.18 m panels, was not available. Outdoor testing eliminated the need to adjust the electrical output of the cells to take into account solar spectrum differences between an indoor solar simulator and outdoor test conditions. Finally, results could be compared to similar panels previously tested outdoors at SNL [6].

The methodology proposed by SNL [7] for outdoor testing was utilized. Each building integrated photovoltaic panel is mounted on an extruded polystyrene insulation board having a nominal thermal resistance of 3.5 m^2 K/W. Prior to testing, the panel is shaded with a reflective cover positioned approximately 75 mm above the photovoltaic panel.

During the tests, the mobile solar tracker facility is operated in the full tracking mode, resulting in the sun's rays being perpendicular to the panel's surface throughout the test. The instrumentation and IV curve tracer are started and the cover used to shade the panel is removed. The IV curve tracer measures the electrical output every minute until the panel approaches a steady-state temperature. The temperatures of the BIPV panel are measured at five locations on the back surface of each BIPV panel. The thermocouples attached to the rear of two centrally located cells with the custom fabricated BIPV panels provide additional temperature measurements.

The tests are conducted when the absolute air mass is as close as possible to the reference value of 1.5, minimizing the need to correct the test data using the air mass function. The measured short-circuit current and maximum power current are adjusted by multiplying by the ratio of the reference irradiance, E_o, (1000 W/m^2) to the measured irradiance and by normalizing the data, using an air mass function, to an absolute air mass of 1.5. The adjusted Isc and Imp for each IV curve is plotted against the average panel temperature as shown in Fig. 2. The slopes of the resulting regressions are the temperature coefficients for I_{sc} and I_{mp}.

The temperature coefficients for the open circuit and maximum power voltage are determined in a similar manner using the same set of IV curves. Unlike the short circuit current and maximum power current, the voltage values are assumed be independent of the solar irradiance level and air mass. King et al. [7] found that there is typically less than a 5% change in the voltage coefficients over a 10-fold change in irradiance—100–1000 W/m^2. The open circuit and maximum power voltage for each IV curve is plotted versus the panel's temperature. The slope of the linear regressions relating the open voltages to panel temperature are the voltage temperature coefficients, Fig. 3.

Air Mass Function. The air mass function used in the IV Curve Tracer photovoltaic model is an attempt to capture the influence of the solar energy's spectral distribution on the conversion efficiency of the photovoltaic cells. The solar spectrum is influenced by a number of factors including the absolute air mass, precipitable water content, turbidity, clouds, aerosol particle size distribution, particulate matter, and ground reflectance [8]. The magnitude of the solar spectrum's effect on the photovoltaic cell's performance depends upon the type of cell technology being utilized. King [9] has found that under clear sky conditions, the majority of the solar spectral influence can be taken into account by considering only the air mass. The relationship between the photovoltaic panel's short circuit current and absolute air mass is defined as the air mass function.

The air mass function for each of the building integrated photovoltaic panels was measured using the methodology proposed by King et al. [10]. The tracking facility is operated in a manner that maintains a zero angle of incidence throughout the day. The curve tracer and instrumentation used to measure the meteorological conditions and the photovoltaic panel's temperature are synchronized and started at sunrise. Data are collected every minute until sunset.

The short-circuit current associated with each IV curve is adjusted to a nominal temperature, T_r, of 25°C and nominal irradiance, E_o, of 1000 W/m^2 using the previously measured short-circuit temperature coefficient,

$$I_{sc}(T_r)=I_{sc}(T)+\frac{E}{E_o}\alpha_{Isc}(T_r-T) \tag{1}$$

The relative short circuit values are subsequently obtained by dividing the temperature adjusted current I_{sc} (T_r) values by the temperature adjusted short circuit current measured at an absolute air mass of 1.5. The air mass is computed using the zenith angle of the sun, Z_s, [10]

$$AM=[\cos(Z_s)+0.5057\cdot(96.080-Z_s)^{-1.634}]^{-1} \tag{2}$$

Finally, the absolute air mass is computed by multiplying the air mass value (Eq. (2)) by the product of the atmospheric pressure at the test site, P, to the atmospheric pressure at sea level, Po

$$AM_a=\frac{P}{P_o}AM \tag{3}$$

The relative short circuit current values versus the absolute air mass for the polycrystalline BIPV panel are plotted in Fig. 4 for three test days. A fourth-order regression is used to determine the coefficients associated with the equation,

$$f(AM_a)=C+C_1\cdot AM_a+C_2\cdot AM_a^2+C_3\cdot AM_a^3+C_4\cdot AM_a^4 \tag{4}$$

It is interesting to note that the measured relative short-circuit current values for various days do not necessarily coincide. This is

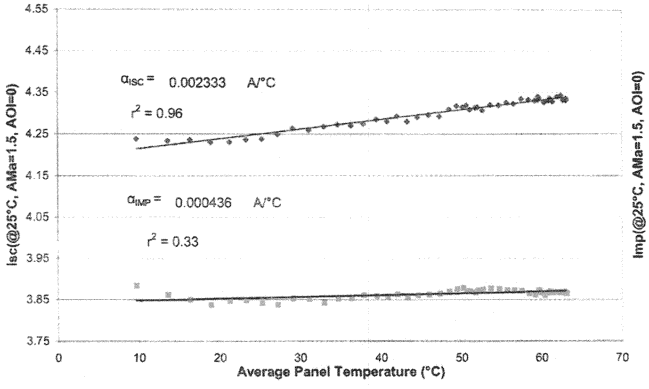

Fig. 2 Polycrystalline BIPV panel I_{sc} and I_{mp} versus panel temperature

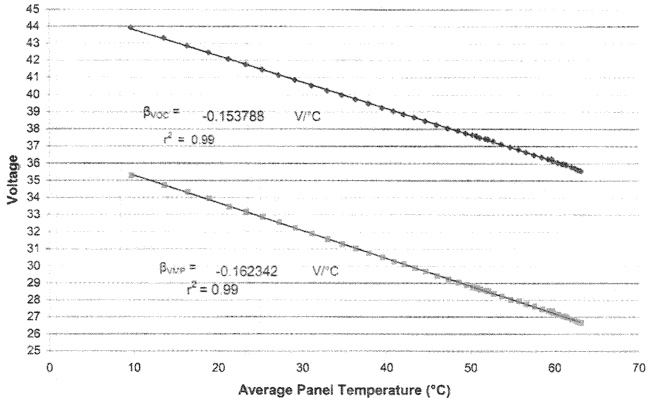

Fig. 3 Polycrystalline BIPV panel V_{oc} and V_{mp} versus temperature

especially notable at air mass values greater than five. It is speculated that although *clear sky* test days were selected, the day-to-day variability in water content, turbidity, particulate matter, and other factors produced the data scatter. Fortuitously, the amount of incident radiation available to a BIPV panel incorporated within a building during the hours at which high values of absolute air mass occur tends to be quite small, and thus, the uncertainty in the air mass function may have a small effect on daily energy production.

Incident Angle Function. The angle defined by the sun's rays and a normal to the photovoltaic panel's surface, is the angle of incidence or incident angle. The angle of incidence is computed using the sun's azimuth and zenith angles, the slope and azimuth angles of the BIPV panel, and the panel's geographical location [11]. The optical properties of the panel's glazing material varies with incident angle. Under clear sky conditions, the *incident angle effect* can be quite pronounced for angles greater than 60 deg. Under uniform diffuse conditions, the angle of incidence does not affect the electrical output of the photovoltaic panel.

The effect of incident angle on the electrical performance of a photovoltaic panel is described by an empirically determined function, f_2 (AOI). The solar tracking facility is used to vary the incident angles of the BIPV panel while capturing its performance using the IV curve tracer. Data are collected at various incident angles with the greatest emphasis on incident angles greater than 60 deg. A normal incidence pyreheliometer, part of NIST's rooftop meteorological station [4] provides independent measurements of the beam irradiance during these tests. The diffuse irradiance in the plane of the BIPV panel is determined using the following equation,

$$E_{diff} = E_{tpoa} - E_{dni} \cos \Theta \tag{5}$$

where E_{tpoa} is the total incident solar radiation, corrected for incident angle, measured in the plane of the BIPV panel using a precision spectral pyranometer, W/m^2; E_{dni} is the beam irradiance measured using a normal incident pyreheliometer tracking the sun, W/m^2; and Θ is the incident angle, deg.

The incident angle function value for each measurement is computed using the procedure developed by King et al. [10],

$$f_2(AOI) = \frac{\dfrac{E_o}{I_{sco}} I_{sc}(AM_a = 1.5,\ T = 25^\circ\mathrm{C}) - E_{diff}}{E_{dni} \cos(\Theta)} \tag{6}$$

Figure 5 is a plot of the resulting incident angle function values for the BIPV panel that incorporates polycrystalline cells. Values resulting from four test days are included. These results are in excellent agreement with measurements reported by King et al. [12].

Normal Operating Cell Temperature. The photovoltaic cells operating temperature is needed in order to translate the performance of the BIPV panels from the standard rating temperature of 25°C to the panels' performance at operating temperatures. The PHANTASM model requires that the user input the nominal operating cell temperature (NOCT) of the photovoltaic panels whereas the PV-Design Pro model predicts cell operating temperature using an empirical correlation [2].

The procedure for determining NOCT temperature is outlined within Appendix A1 of ASTM Standard E 1036M [5]. NOCT is defined as the temperature of the solar cells when they are subjected to a solar irradiance of 800 W/m^2, a 1-m/s wind speed, and a surrounding ambient temperature of 20°C. The photovoltaic panel is mounted such that it is normal to the sun at solar noon. The panels' temperature is measured for a period beginning at least 4 hr before solar noon and continuing for at least 4 hr after solar noon. During the test, the panel is not connected to an electrical load. The wind speed and direction, solar irradiance, and ambient temperature are monitored throughout the test. ASTM E 1036M specifies that the wind direction must be "predominantly either northerly or southerly."

The data are filtered to include only measurements consistent with wind speeds between 0.25 m/s and 1.75 m/s and with gusts less than 4 m/s for a period of at least 5 min prior to the measurement. The ambient temperature must be between 5°C and 35°C. The filtered data set is used to produce a plot of the difference between the photovoltaic cell's temperature and ambient temperature versus solar irradiance. Using this plot the NOCT is determined for an incident irradiance of 800 W/m^2 and 20°C ambient temperature. Finally, a correction factor is added to this value to translate the measured NOCT from the test conditions to ambient conditions of 20°C and 1 m/s.

Electrical Performance at Standard Rating Conditions. A required input to the computer simulation tools is the electrical performance of each BIPV panel at a specified set of test conditions, *Standard Reporting Conditions* (SRC). Typically an irradiance level of 1000 W/m^2, one of two standard solar spectral distributions, a cell temperature of 25°C, and a 0-deg angle of irradiance have been specified. These conditions have been adopted in this paper as the standard rating conditions with the exception of the standard solar spectrum. In the values reported within this paper, the BIPV panels' performance at an absolute air mass of 1.5 is used in lieu of a standard solar spectrum.

Each BIPV panels' performance at this set of rating conditions is determined using the procedures developed by King et al. [9,12]. Using the mobile solar tracker to maintain the sun's rays perpendicular to the front surface of the panel ($AOI = 0$), the curve tracer is used to collect IV curves under clear sky conditions. The resulting short-circuit current values are corrected to an

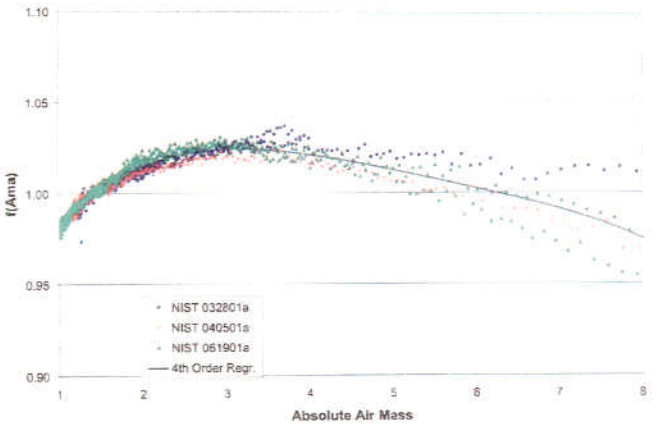

Fig. 4 Polycrystalline BIPV panel air mass function

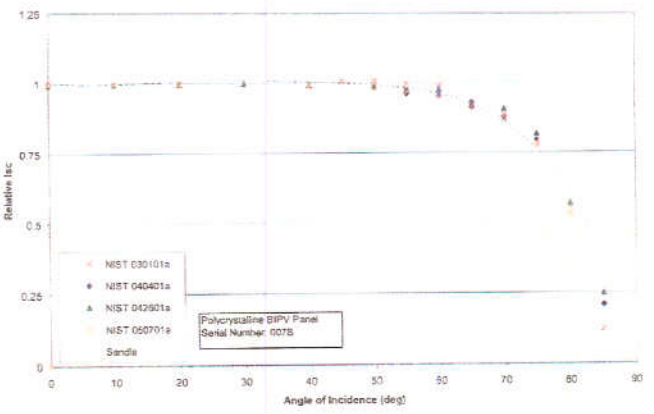

Fig. 5 Incident angle response for polycrystalline BIPV panel

Table 2 Measured Temperature Coefficients

Monocrystalline BIPV Panel	Test Date		090501a	091101a	091501a	091501b	091701a	Average	Std. Deviation
	α-Isc	A/°C	0.001868	0.001756	0.001776	0.001657	0.001707	0.001753	0.0000792
		1/°C	0.000427	0.000401	0.000406	0.000379	0.000390	0.000401	0.0000181
	α-Imp	A/°C	−0.001327	−0.001455	−0.001484	−0.001504	−0.001947	−0.001543	0.0002362
		1/°C	−0.000335	−0.000367	−0.000375	−0.000380	−0.000492	−0.000390	0.0000596
	β-Voc	V/°C	−0.157857	−0.149294	−0.146758	−0.155610	−0.152309	−0.152366	0.0045157
		1/°C	−0.003677	−0.003478	−0.003419	−0.003625	−0.003548	−0.003549	0.0001052
	β-Vmp	V/°C	−0.160084	−0.151999	−0.149460	−0.155116	−0.151231	−0.153578	0.0041731
		1/°C	−0.004753	−0.004513	−0.004438	−0.004606	−0.004490	−0.004560	0.0001239

Polycrystalline BIPV Panel	Test Date		030801a	042601a	050701a	Average	Std. Deviation
	α-Isc	A/°C	0.002299	0.002502	0.002341	0.002380	0.0001071
		1/°C	0.000541	0.000589	0.000551	0.000560	0.0000252
	α-Imp	A/°C	0.000404	0.000161	−0.000031	0.000178	0.0002179
		1/°C	0.000106	0.000042	−0.000008	0.000047	0.0000571
	β-Voc	V/°C	−0.153788	−0.152396	−0.152209	−0.152798	0.0008626
		1/°C	−0.003706	−0.003672	−0.003668	−0.003682	0.0000208
	β-Vmp	V/°C	−0.162342	−0.157700	−0.157306	−0.159116	0.0028010
		1/°C	−0.004928	−0.004787	−0.004775	−0.004830	0.0000850

Silicon Film BIPV Panel	Test Date		062501a	062601a	070201a	070601a	Average	Std. Deviation
	α-Isc	A/°C	0.005756	0.004502	0.004182	0.004294	0.004683	0.0007273
		1/°C	0.001126	0.000880	0.000818	0.000840	0.000916	0.0001422
	α-Imp	A/°C	0.002037	0.001250	0.001467	0.001665	0.001605	0.0003344
		1/°C	0.000454	0.000279	0.000327	0.000371	0.000358	0.0000745
	β-Voc	V/°C	−0.129543	−0.132529	−0.129318	−0.128426	−0.129954	0.0017832
		1/°C	−0.004374	−0.004475	−0.004367	−0.004337	−0.004388	0.0000602
	β-Vmp	V/°C	−0.128977	−0.132790	−0.130170	−0.129611	−0.130387	0.0016744
		1/°C	−0.005568	−0.005732	−0.005619	−0.005595	−0.005629	0.0000723

Triple-Junction Amorphous BIPV Panel	Test Date		100501a	100501b	101101a	101501b	101501c	101501e	Average	Std. Deviation
	α-Isc	A/°C	0.005272	0.005403	0.004942	0.005852	0.006076	0.006094	0.005606	0.0004716
		1/°C	0.001187	0.001217	0.001113	0.001318	0.001368	0.001372	0.001263	0.0001062
	α-Imp	A/°C	0.006675	0.007014	0.006358	0.007392	0.007873	0.008773	0.007348	0.0008779
		1/°C	0.001848	0.001941	0.001760	0.002046	0.002179	0.002428	0.002034	0.0002430
	β-Voc	V/°C	−0.091300	−0.097684	−0.090912	−0.088250	−0.093312	−0.097150	−0.093102	0.0037149
		1/°C	−0.003943	−0.004218	−0.003926	−0.003811	−0.004030	−0.004195	−0.004021	0.0001604
	β-Vmp	V/°C	−0.049692	−0.052583	−0.045426	−0.042296	−0.049436	−0.046943	−0.047729	0.0036267
		1/°C	−0.003099	−0.003279	−0.002833	−0.002637	−0.003083	−0.002927	−0.002976	0.0002261

absolute air mass of 1.5 and a 25°C cell temperature using the previously determined air mass function and temperature coefficients. The resulting I_{sc} values are plotted versus the coincident solar irradiance striking the panel. A regression through the data is used to predict the short circuit current at of 1000 W/m^2, denoted I_{sco}.

In a similar manner, the measured maximum power current values are corrected to an absolute air mass of 1.5 and 25°C cell temperature. The resulting values are plotted versus the effective irradiance. The effective irradiance is defined as,

$$E_e = \frac{I_{sc}(E, T_c = T_r, AM_a, AOI)}{I_{sco}} \tag{7}$$

where the numerator represents the temperature adjusted measured short-circuit current and the denominator is the short-circuit current of the panel at the standard rating conditions. The maximum power current corresponding to an effective irradiance of unity is the maximum power current at standard rating conditions, I_{mpo}.

The open circuit voltage and maximum power voltage measurements associated with each IV curve are plotted versus the natural logarithm of the effective irradiance values. Using a linear regression in the case of the open circuit voltage values, and a second order polynomial in the case of the maximum power voltage values, the open circuit voltage and maximum power voltage values are determined at an effective irradiance of 1.0.

Test Results

Results from tests conducted using the NIST solar tracking test facility are summarized in the following sections. In addition to the NIST results, the measurements are compared to data from the manufacturers and Sandia National Laboratories.

Temperature Coefficients. Table 2 is a compilation of the temperature coefficients, α_{isc}, α_{imp}, β_{voc}, and β_{vmp} measured in accordance with the previously described procedures. Two sets of units are associated with each coefficient. The test procedure produces results in units normally used within the photovoltaic industry, A/°C or V/°C. Unfortunately results presented in these units are not readily compared to temperature coefficients for panels that may use identical cells but differ in the number of cells or the manner in which the cells are interconnected.

In order to address this issue and to facilitate comparisons, the current and voltage temperature coefficients are divided by the corresponding current or voltage values (I_{sco}, I_{mpo}, V_{oco}, and V_{mpo}), at standard rating conditions. If the temperature coefficients of a BIPV panel using identical cells but having a different electrical configuration were needed, the normalized temperature coefficients, (1/°C) could be multiplied by the appropriate value (I_{sc}, I_{mp}, V_{oc}, and V_{mp}) of the panel for which the coefficients are desired.

For any given BIPV panel, test-to-test variations exist in the measured values, Table 2. The variations in temperature coefficients for current tend to be greater than those associated with

Table 3 Summary of measured building integrated photovoltaic panel

Reference Cond.		Silicon Film			Mono Crystalline			Polycrystalline			Triple Junction Amorphous		
		Manufacturer	NIST	SNL	Manufacturer	NIST	SNL	Manufacturer	NIST	SNL	Manufacturer	NIST	SNL
P_{mpo}	(W)	125.94	103.96		149.60	133.40		128.10	125.78		64.02	57.04	
I_{sco}	(A)	5.80	5.11		4.80	4.37		4.00	4.25		4.80	4.44	
V_{oco}	(V)	30.66	29.61		43.40	42.93		42.60	41.50		23.80	23.16	
I_{mpo}	(A)	5.20	4.49		4.40	3.96		3.66	3.82		3.88	3.61	
V_{mpo}	(V)	24.22	23.17		34.00	33.68		35.00	32.94		16.50	16.04	
NOCT	(°C)	47	44		45			47			42		
Temperature Coefficients													
α_{Isc}	(A/°C)	0.00400	0.00468		0.00206	0.00175		0.00260	0.00238		0.00480	0.00561	0.00424
α_{Isc}	(1/°C)	0.000690	0.000916	0.000760	0.000429	0.000401	0.000370	0.000650	0.000560	0.000512	0.001000	0.001263	0.000850
α_{Imp}	(A/°C)		0.00160			−0.00154			0.00018		0.00388	0.00735	0.00480
α_{Imp}	(1/°C)		0.000358	0.000030		−0.000390	−0.000395		0.000047	−0.000148	0.001000	0.002034	0.001187
β_{Voc}	(V/°C)	−0.12600	−0.12995		−0.15400	−0.15237		−0.16000	−0.15280		−0.09044	−0.09310	−0.09767
β_{Voc}	(1/°C)	−0.004110	−0.004388	−0.004384	−0.003548	−0.003549	−0.004038	−0.003756	−0.003682	−0.003720	−0.003800	−0.004021	−0.004386
β_{Vmp}	(V/°C)		−0.13039			−0.15358			−0.15912		−0.05115	−0.04773	−0.05167
β_{Vmp}	(1/°C)		−0.005629	−0.005434		−0.004560	−0.005172		−0.004830	−0.004779	−0.003100	−0.002976	−0.003257
Coefficients for Air Mass and Angle of Incidence Functions													
f(AMa)	Cnst		0.938110	0.928000		0.935823	0.938000		0.918093	0.913000		1.10044085	1.047
	Ama		0.062191	0.073144		0.054289	0.054228		0.086257	0.079168		−0.06142323	0.00082115
	AMa^2		−0.015021	−0.019427		−0.008677	−0.009903		−0.024459	−0.015975		−0.00442732	−0.0259
	AMa^3		0.001217	0.001751		0.000527	0.000730		0.002816	0.001306		0.000631504	0.0031736
	AMa^4		−0.000034	−0.000051		−0.000011	−0.000019		−0.000126	−0.000037		−1.9184E-05	−0.00011026
f(AOI)	Cnst		0.998980	1.000000		1.000341	1.000000		0.998515	1.000000		1.001845	1.000000
	AOI		−0.006098	−0.002438		−0.005557	−0.002438		−0.012122	−0.002438		−0.005648	−0.00502
	AOI^2		8.117E-04	0.000310		6.553E-04	0.000310		1.440E-03	0.000310		7.254E-04	0.0005842
	AOI^3		−3.376E-05	−1.246E-05		−2.730E-05	−1.246E-05		−5.576E-05	−1.246E-05		−2.916E-05	−0.000023
	AOI^4		5.647E-07	2.112E-07		4.641E-07	2.112E-07		8.779E-07	2.112E-07		4.696E-07	3.826E-07
	AOI^5		−3.371E-09	−1.359E-09		−2.806E-09	−1.359E-09		−4.919E-09	−1.359E-09		−2.739E-09	−2.31E-09

The following values of uncertainty associated with the measurements in Table 3 represent the expanded uncertainty using a coverage factor of 2.
P_{mpo} -±1% α_{Isc} ±6% I_{sco} -±1% α_{Imp} ±20%
V_{oco} -±1% β_{Voc} ±1% I_{mpo} -±1% β_{Vmp} ±1%
V_{mpo} -±1%

voltage. The test-to-test variation is partially attributed to variations in spectral content, irradiance level, and temperature associated with outdoor testing [13].

It is interesting to note that although the short circuit current increases with temperature for all four panels, the maximum power current increases with temperature for the polycrystalline, silicon film, and triple junction amorphous panels while decreasing with temperature for the mono-crystalline panel.

The NIST measured temperature coefficients are compared to values within the manufacturer's literature and measurements at SNL for modules that incorporate identical cells within Table 3. The manufacturer's literature values were obtained from data sheets that accompanied the cells used in the fabrication of the custom BIPV panels, or from literature associated with a photovoltaic module using identical cells. Agreement between the manufacturer's data, NIST values, and measurements at SNL for the open circuit and maximum power voltage temperature coefficients is good. In general, agreement between the three values of the temperature coefficients associated with short circuit and maximum power current is good with the exception of the NIST measured values associated with triple junction amorphous panel and the maximum power coefficients associated with the polycrystalline panel.

Air Mass Functions. The measured air mass response for the monocrystalline, polycrystalline, silicon film, and triple junction amorphous silicon BIPV panels are shown in Fig. 6. It is interesting to note that the relative air mass response is similar for the BIPV panels that utilize the monocrystalline, polycrystalline, and silicon film cells. Air mass has a much greater effect on the triple junction amorphous BIPV panel than the other three panels. At an absolute air mass of six, the relative air mass response for the panel using the triple-junction amorphous technology is approximately 70% of that exhibited by the BIPV panels utilizing the other cell technologies. The significantly lower air mass response exhibited by the triple-junction amorphous panel, at air mass values greater than 1.5, is due to the fact that amorphous silicon cells are less responsive, compared to the other cell technologies, to the portion of the solar spectrum with wavelengths greater than 900 nm. As the absolute air mass increases, the solar spectrum contains a greater percentage of wavelengths above 900 nm resulting in the significant drop off exhibited in Fig. 6. Excellent agreement exists between the air mass functions measured at NIST and those published by SNL for modules that utilize the same cell technologies with the exception of the BIPV panel that incorporates polycrystalline cells, Fig. 6. The NIST measured results for the polycrystalline BIPV panel deviates from the SNL results as the absolute air mass increases. The reason for this discrepancy is unknown.

Incident Angle Functions. The coefficients resulting from a fifth order curve fit to the data sets in Fig. 7, to the incident angle for each BIPV panel are listed in Table 3. SNL data for modules utilizing identical cell technologies is included for comparison.

It is interesting to note that the incident angle response for the mono-crystalline, polycrystalline, and silicon film BIPV panels are almost identical. This is attributed to the fact that the glazing associated with these panels is identical, 6-mm low iron glass. The triple junction amorphous panel uses a two mil *Tefzel glazing and exhibits a somewhat different response to the angle of incidence.

Nominal Operating Cell Temperature. Table 4 summarizes the measured nominal operating cell temperatures (NOCT) of the BIPV panels. Two NOCT values are tabulated for each of the four cell technologies, one for an un-insulated panel and a second value for a panel with extruded polystyrene, having a nominal thickness and thermal resistance of 10.16 cm and 3.5 m^2 K/W, respectively, attached to its rear surface. These two test conditions were chosen to replicate the installation of the panels within NIST's BIPV "test bed" [1,4].

The measured NOCT values for the un-insulated BIPV panels using mono-crystalline, polycrystalline, and silicon film cells are within 1°C of each other. Attachment of the insulation to the rear surface of each of these panels elevated the NOCT values by 21–23°C. Since these three panels are identical, with the exception of the cell technology, it is not surprising that the resulting NOCT values are in close agreement. The triple junction amorphous panel is a commercially available module that bares little resemblance to the other three panels. Thus, the significantly different NOCT values for the triple-junction amorphous panel are not unexpected.

The uncertainty associated with the instrumentation used to measure the NOCT temperatures is estimated to be ±0.4°C. However, due to the inherent difficulties in measuring wind velocity and direction at the panel's surface in conjunction with the thermal mass associated with the panel, it is unlikely that the values in Table 4 represent true NOCT temperatures better than ±3.0°C.

Electrical Performance at Standard Rating Conditions. The current and voltage values for each photovoltaic panel at standard rating conditions are given in Table 3. These values include the maximum power output (P_{mpo}), the current and voltage at the maximum power point (I_{mpo} and V_{mpo}, respectively) the short circuit current (I_{sco}) and the voltage at open circuit conditions (V_{oco}). The custom fabricated BIPV panels are exact duplicates of the panels used within NIST's BIPV "test bed." The values listed in Table 3 are for a single triple-junction amorphous panel are for a single module, while the NIST BIPV "test bed"

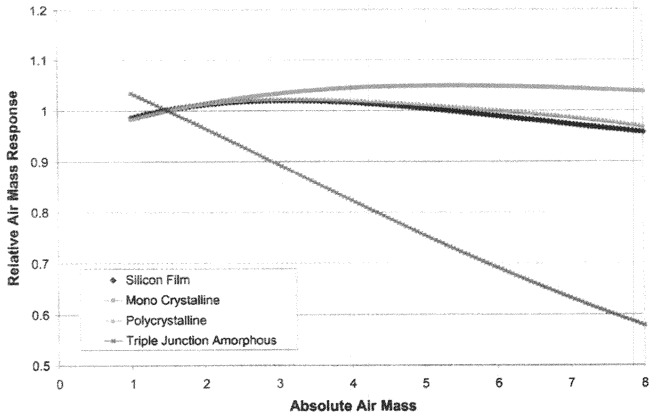

Fig. 6 Air mass response function for BIPV Panels

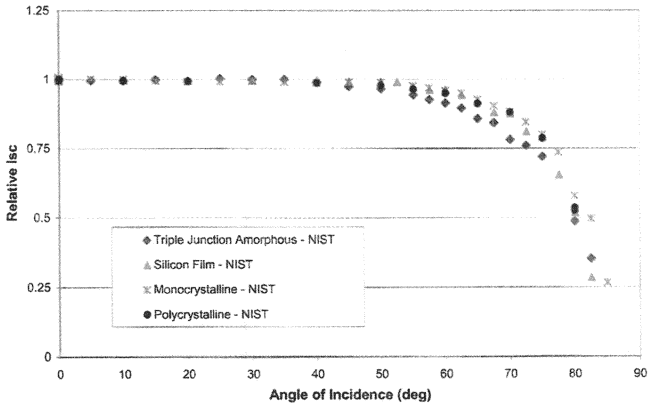

Fig. 7 Angle of incidence function for BIPV panels

Table 4 NOCT summary (°C)

	Silicon Film	Mono-Crystalline	Poly Crystalline	Triple Junction Amorphous
Un-insulated Panel	43.0	43.7	43.3	37.9
Insulated Panel	64.7	66.7	65.5	55.3

uses two of these connected in series. The amorphous silicon panel is an actual panel removed from the "test bed" after approximately 18 months of exposure.

The performance values in Table 3 denoted "Manufacturer" were derived in the following manner. Each of the manufacturers that provided cells for the custom fabricated BIPV panels also produces complete modules. Product information from the manufacturer's specification sheet for a module using the same cell technology and as close, as possible, the power rating of the BIPV panel was selected. The current, voltage, and power values from the module specification sheets were scaled appropriately for differences in the number of cells and electrical configuration. Close agreement between the NIST measurements for the BIPV modules and those derived from the specification sheets is not expected. Differences are attributed to variations in the glazings' solar transmittance, cell performance, and manufacturing procedures.

As expected, the current output of the silicon film panel is greater than that of the mono-crystalline or polycrystalline panels due to the larger cell size, 150 mm×150 mm versus 125 mm×125 mm. As a result of 72 cells being connected in series for the mono-crystalline and polycrystalline panels, compared to 56 for the silicon film panel, the voltage measurements associated with these two panels are significantly higher than those for the silicon film panel.

Summary

A series of tests to characterize the performance of three custom fabricated BIPV panels and one commercially available photovoltaic panel have been completed.

Tests were conducted to determine the response of each panel to changes in cell temperature, absolute air mass and angle of incidence. The performance of each panel at Standard Rating Conditions was determined.

The measured temperature coefficients were generally in good agreement with data provided by the manufacturers and SNL. The three custom fabricated BIPV panels exhibited similar responses to changes in absolute air mass and angle of incidence. The response of the fourth panel, the triple junction amorphous panel, to changes in absolute air mass and angle of incidence was distinctly different from the other three panels.

The nominal operating cell temperatures for the four panels were measured with and without thermal insulation attached to the panels' rear surface. The addition of insulation increased the NOCT temperatures by approximately 21°C for the custom fabricated panels and 17°C in the case of the triple junction amorphous silicon panel. The un-insulated and insulated amorphous panel's NOCT temperatures are approximately 5°C and 10°C less than the corresponding temperatures for the custom fabricated panels.

The parameters that have resulted from this work are being incorporated into the IV Curve Tracer and PHANTASM models. These models are being used to predict the annual performance of identical panels installed in NIST's BIPV "test bed."

Acknowledgments

NIST's Building and Fire Research Laboratory and Advanced Technology Program as well as the California Energy Commission support this research. The assistance of David L. King and his colleagues at Sandia National Laboratories is greatly appreciated. They have provided continued and unwavering support throughout this project. Special thanks to Pete DeNapoli, Siemens Solar Systems, John Wolgemuth, BP/Solarex, and Jake Brown of Solar Building Systems for fielding numerous technical questions. Stanley Morehouse constructed the solar tracker test facility used throughout this investigation. Stanley Morehouse, Daniel Vennetti, and David Frankford conducted the various tests described within this paper. The paper was typed and edited by Paula Svincek.

References

[1] Fanney, A. H., Dougherty, B. P., and Davis, M. W., 2001, "Measured Performance of Building Integrated Photovoltaic Panels," ASME J. Sol. Energy Eng., **123**(3), pp. 187–193.

[2] PV-Design Pro, 2000, Solar Design Studio, v4.0, Maui Solar Energy Software Corp., Haiku, HI.

[3] PHotovoltaic ANalysis and TrAnsient Simulation Method (PHANTASM), 1999, Building Integrated Photovoltaic Simulation Software, Solar Energy Laboratory, Univ. of Wisconsin, Madison, WI.

[4] Fanney, A. H., and Dougherty, B. P., 2001, "Building Integrated Photovoltaic Test Facility," ASME J. Sol. Energy Eng., **123**(3), pp. 200–210.

[5] ASTM "E 1036M, 2001, "Standard Test Methods for Electrical Performance of Nonconcentrator Terrestrial Photovoltaic Modules and Arrays Using Reference Cells," Annual Book of ASTM Standards, Vol. 12.02.

[6] "Database of Photovoltaic Module Performance Parameters," 2000, http://www.sandia.gov/pv/pvc.htm

[7] King, D. L., Kratochvil, J. A., and Boyson, W. E, 1997, "Temperature Coefficients for PV Modules and Arrays: Measurement Methods, Difficulties, and Results," *Proc. 26th IEEE Photovoltaic Specialists Conf.*, Anaheim, CA, pp. 1183–1186.

[8] Zanesco, L., and Krenzinger, A., 1993, "The Effects of Atmospheric Parameters on the Global Solar Irradiance and on the Current of a Silicon Solar Cell," Prog. Photovoltaics, **1**(3), pp. 169–179.

[9] King, D. L., 1996, "Photovoltaic Module and Array Performance Characterization Methods for all System Operating Conditions," *Proc. NREL/SNL Photovoltaics Program Review*, AIP Press, Lakewood, CO, pp. 347–368.

[10] King, D. L., Kratochvil, J. A., and Boyson, W. E, 1997, "Measuring Solar Spectral and Angle-of-Incidence Effects on Photovoltaic Modules and Solar Irradiance Sensors," *Proc. 26th IEEE Photovoltaic Specialists Conf.*, Anaheim, CA, pp. 1113–1116.

[11] Duffie, J. A., and Beckman, W. A., 1991, *Solar Engineering of Thermal Processes*, John Wiley and Sons, New York.

[12] King, D. L., Kratochvil, J. A., and Boyson, W. E, 1998, "Field Experience with a New Performance Characterization Procedure for Photovoltaic Arrays," *Proc. 2nd World Conf. and Exhibition on Photovoltaic Solar Energy Conversion*, Vienna, Austria.

[13] Emery, K., Burdick, J., Field, H., Kroposki, B., Strand, T., and Wanlass, M., 1996, "Temperature Dependence of Photovoltaic Cells, Modules and Systems," *Proc. 25th IEEE PVSC*, Washington, DC, pp. 1275–1278.